JOURNAL OF COLLOID AND INTERFACE SCIENCE 160, 236–242 (1993)

Analytical Expressions for the Shape of Small Drops and Bubbles

P. A. KRALCHEVSKY,*[1] A. S. DIMITROV,†[2] AND K. NAGAYAMA†

* *Laboratory of Thermodynamics and Physicochemical Hydrodynamics, University of Sofia, Faculty of Chemistry, Sofia 1126, Bulgaria; and † Protein Array Project, ERATO, JRDC, 5-9-1 Tokodai, Tsukuba, 300-26 Japan*

Received October 12, 1992; accepted April 5, 1993

Analytical expressions describing the shape of small axisymmetric sessile and pendant drops or bubbles are derived. The expressions represent compound asymptotic expansions for small values of the Bond number. The accuracy of the asymptotic expansions is examined against the exact computer solutions of the Laplace equation of capillarity. The derived equations can be useful in interpreting the data from different methods of contact angle measurement with sessile or pendant fluid particles.

1. INTRODUCTION

Knowledge of the shape of axisymmetrical sessile and pendant drops or bubbles is important for different experimental methods for surface tension and contact angle measurement (1–8). Since the Laplace equation of capillarity has no analytical solution in this case, computer solutions are frequently used. In the case of small or large values of the Bond number, approximate analytical expressions can be derived—see, e.g., Refs. (2, 9, 10). If available, such expressions help to speed up the computer calculations, especially when experimental data for the interfacial profile are processed.

In a previous paper (10) outer and inner asymptotic expansions were obtained describing the profiles of small sessile and pendant drops or bubbles. In this case the drops (bubbles) represent parts of slightly deformed spheres (small Bond numbers). That is why the zeroth-order approximation for the interfacial profile is a sphere and the higher-order terms with respect to the Bond number account for the deformation due to gravity. Unfortunately, the asymptotic expansions, derived in Ref. (10), turned out to be nonuniformly valid irrespective of the large domain of validity of the outer expansion. Our aim in the present study is to obtain an asymptotic expansion which is uniformly valid for surface slopes from 0° up to 180°, and to check the accuracy of this expansion against the exact numerical data from the computer integration. For that purpose we make use of the method of the compound asymptotic expansion—see, e.g., Ref. (11).

2. COMPOUND ASYMPTOTIC EXPANSION

For the sake of convenience we use here the same notation and the same choice of the coordinate system as in Ref. (10). In particular, the coordinate origin is chosen at the apex of the drop or bubble, i.e., the point where the two principal radii of curvature are equal to each other—Fig. 1. The radius of curvature at this special point is denoted by b. The z-axis coincides with the axis of revolution of the interface and is directed toward the interior of the fluid particle (drop or bubble). In terms of the dimensionless variables

$$\bar{x} = \frac{x}{b}, \quad \bar{z} = \frac{z}{b}, \quad \beta = \frac{\Delta\rho g b^2}{\sigma} \qquad [1]$$

(β is the Bond number), the Laplace equation of capillarity takes the form (4, 10)

$$\frac{1}{\bar{x}}\frac{d}{d\bar{x}}(\bar{x}\sin\varphi) = 2 + \epsilon\beta\bar{z} \qquad [2]$$

$$\frac{d\bar{z}}{d\varphi} = -\frac{d\bar{x}}{d\varphi}\tan\varphi. \qquad [3]$$

Here $\epsilon = 1$ for a sessile interface and $\epsilon = -1$ for a pendant interface; $\Delta\rho$ is the density difference between the heavier and the lighter phases ($\Delta\rho > 0$), σ is surface tension, and g is gravity acceleration; and the angle φ characterizes the slope of the interface: φ equals π at the particle apex (where $z = 0$) and then φ decreases with the increase of z—cf. Fig. 1. Our aim is to find the profile of the fluid particle in a parametric form,

$$\bar{x} = \bar{x}(\varphi), \quad \bar{z} = \bar{z}(\varphi), \qquad [4]$$

by solving Eqs. [2] and [3] with the boundary conditions

$$\bar{x} = 0, \quad \bar{z} = 0 \quad \text{at} \quad \varphi = \pi. \qquad [5]$$

[1] To whom correspondence should be addressed.
[2] On temporary leave from the University of Sofia.

0021-9797/93 $5.00

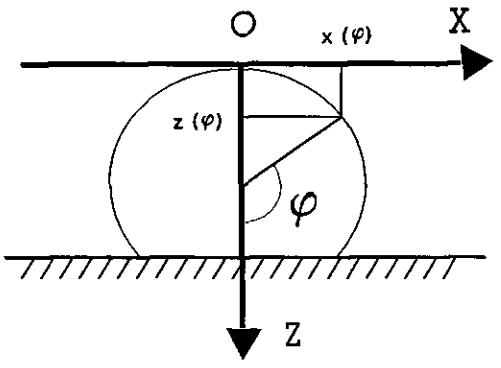

FIG. 1. Sketch of an axisymmetric fluid particle attached to an interface.

The method of the matched outer and inner asymptotic expansions was used to solve this problem. The outer expansion describes the surface profile in the region closer to the fluid particle apex, whereas the inner expansion describes the region of small φ ($\varphi \to 0$). The outer expansions for $\bar{x}(\varphi)$ and $\bar{z}(\varphi)$ read (10)

$$\bar{x}^{\text{out}} = \sin\varphi + \beta\epsilon\left(\frac{1}{3}\cot\frac{\varphi}{2} - \frac{1}{6}\sin 2\varphi - \frac{1}{2}\sin\varphi\right) + \beta^2\left\{\left[\frac{3}{4} + \frac{1}{2}\cos\varphi - \frac{2}{9}\sin^2\varphi - \frac{1}{3}\ln\left(\sin\frac{\varphi}{2}\right)\right]\sin\varphi - \frac{1}{2}\left(1 + \frac{1}{9}\cot^2\frac{\varphi}{2}\right)\cot\frac{\varphi}{2}\right\} + O(\beta^3) \quad [6]$$

$$\bar{z}^{\text{out}} = 1 + \cos\varphi + \beta\epsilon\left[\frac{1}{3}\sin^2\varphi + \frac{2}{3}\ln\left(\sin\frac{\varphi}{2}\right) - \frac{1}{2}(1 + \cos\varphi)\right] + O(\beta^2). \quad [7]$$

For $\beta \ll 1$ Eqs. [6] and [7] were found to describe the shape of the interface with very good accuracy for $15° < \varphi \leqslant 180°$. However, for $\varphi < 15°$ the accuracy fast decreases (see Fig. 3 in Ref. (10)) and both Eqs. [6] and [7] exhibit divergence for $\varphi \to 0$.

The inner expansions for $\bar{x}(\varphi)$ and $\bar{z}(\varphi)$, which are to be used in the region $0 \leqslant \varphi \leqslant 15°$, have the form

$$\bar{x}^{\text{in}} = u - \frac{27u^7 + 108\epsilon\beta u^5 + 144\beta^2u^3 - 8\epsilon\beta^3 u}{54(3u^4 + 2\epsilon\beta u^2)} + O(\beta^2), \quad [8]$$

$$\bar{z}^{\text{in}} = 2 - \frac{1}{2}\varphi u + \frac{2}{3}\beta\epsilon\ln\frac{u}{2e} + O(\beta^2), \quad [9]$$

where e is the Napier number ($\ln e = 1$) and

$$u = \frac{1}{2}\left(\varphi + \eta\sqrt{\varphi^2 + \frac{8}{3}\epsilon\beta}\right), \quad \eta = \pm 1. \quad [10]$$

For *pendant* interfaces $\epsilon = -1$ and the angle φ has a minimum value $\varphi = \varphi_i$ corresponding to the inflectional point of the surface profile $z = z(x)$. Since the inflectional point also corresponds to zero under the square root in Eq. [10], one finds

$$\varphi_i^2 = \frac{8}{3}\beta + O(\beta^2). \quad [11]$$

Besides, for the sessile interface ($\epsilon = 1$) one has identically $\eta = 1$ in Eq. [10]; for the pendant interface $\eta = 1$ for $z < z(\varphi_i)$ and $\eta = -1$ for $z > z(\varphi_i)$.

It should be noted that Eq. [8] was derived in Ref. (10) for the case of a sessile interface. We derived Eq. [9] by using the same asymptotic procedure, which is described in Ref. (10). The only difference is that we used a modified version of Eq. [24] in Ref. (10):

$$\bar{z}(\tilde{\varphi}, \beta) = \tilde{z}_0(\tilde{\varphi}) + (\beta\ln\beta)\tilde{z}_1(\tilde{\varphi}) + \beta\tilde{z}_2(\tilde{\varphi}) + \cdots, \quad \tilde{\varphi} = \frac{\varphi}{\sqrt{\beta}}. \quad [12]$$

The integration constants in Eqs. [8] and [9] were determined in accordance with the method of the matched asymptotic expansions, i.e., in such a way that the outer expansion of the inner solution was equal to the inner expansion of the outer solution (see, e.g., Ref. (11)]:

$$(\bar{x}^{\text{in}})^{\text{out}} = (\bar{x}^{\text{out}})^{\text{in}}; \quad (\bar{z}^{\text{in}})^{\text{out}} = (\bar{z}^{\text{out}})^{\text{in}}. \quad [13]$$

Here

$$(\bar{x}^{\text{out}})^{\text{in}} = \varphi - \frac{\varphi^3}{6} + \beta\epsilon\left(\frac{2}{3}\frac{1}{\varphi} - \frac{8}{9}\varphi\right) - \beta^2\left(\frac{4}{9}\frac{1}{\varphi^3} + \frac{8}{9}\frac{1}{\varphi}\right), \quad [14]$$

$$(\bar{z}^{\text{out}})^{\text{in}} = 2 - \frac{\varphi^2}{2} + \beta\epsilon\left(\frac{2}{3}\ln\frac{\varphi}{2} - 1\right). \quad [15]$$

Equations [14] and [15] can be derived from Eqs. [6] and [7] by expanding in series for small φ and keeping the two leading terms of the expansions.

Finally, in accordance with the asymptotic procedure (11) one can formulate the compound solution, which is uniformly valid in the outer and inner regions:

$$\frac{x(\varphi)}{b} = \bar{x} = \bar{x}^{\text{out}} + \bar{x}^{\text{in}} - (\bar{x}^{\text{out}})^{\text{in}} \quad [16]$$

$$\frac{z(\varphi)}{b} = \bar{z} = \bar{z}^{\text{out}} + \bar{z}^{\text{in}} - (\bar{z}^{\text{out}})^{\text{in}}. \quad [17]$$

Thus to calculate the dependencies $x(\varphi)$ and $z(\varphi)$ from Eqs. [16] and [17] one substitutes $\bar{x}^{out}$ and $\bar{z}^{out}$ from Eqs. [6] and [7], $\bar{x}^{in}$ and $\bar{z}^{in}$ from Eqs. [8] and [9], and $(\bar{x}^{out})^{in}$ and $(\bar{z}^{out})^{in}$ from Eqs. [14] and [15]. The functions $x(\varphi)$ and $z(\varphi)$ calculated in this way are compared in the next section with the exact computer solution of the Laplace equation, Eqs. [2] and [3], for different values of the Bond number, β.

In the end of this section it is to be noted that in the compound solutions, Eqs. [16] and [17], the divergent terms in $\bar{x}^{out}$ and $\bar{z}^{out}$ for $\varphi \to 0$ are exactly canceled by the respective divergent terms in $(\bar{x}^{out})^{in}$ and $(\bar{z}^{out})^{in}$. Note also that when using Eqs. [8], [9], [14], and [15] one must express angle φ in radians.

3. NUMERICAL RESULTS AND DISCUSSION

Let us define the relative errors of Eqs. [16] and [17]:

$$\delta_x = \frac{\bar{x}(\varphi, \beta) - \bar{x}_{ex}(\varphi, \beta)}{\bar{x}_{ex}(\varphi, \beta)} \qquad [18]$$

$$\delta_z = \frac{\bar{z}(\varphi, \beta) - \bar{z}_{ex}(\varphi, \beta)}{\bar{z}_{ex}(\varphi, \beta)}. \qquad [19]$$

Here $\bar{x}(\varphi, \beta)$ and $\bar{z}(\varphi, \beta)$ are determined from the asymptotic equations and $\bar{x}_{ex}(\varphi, \beta)$ and $\bar{z}_{ex}(\varphi, \beta)$ are the exact values of these functions obtained by numerical integration of the Laplace equation—Eqs. [2] and [3]. To carry out the numerical integration we used the standard Runge–Kutta–Felberg method (RKF45)—see, e.g., Ref. (12). The integration starts from the fluid particle apex ($x = 0$, $z = 0$, $\varphi = \pi$) with appropriate increments in φ up to some given value of φ. If one fixes the relative error δ_x or δ_z, one can calculate by means of Eqs. [18] or [19] the curves of constant error $\beta = \beta(\varphi)$.

(a) Sessile Interface ($\epsilon = 1$; $\eta = 1$)

The relative errors δ_x and δ_z calculated by means of Eqs. [18] and [19] are shown in Fig. 2 as functions of the running slope angle φ. The solid lines represent the relative errors of the compound solution, Eq. [16] or [17]. The respective values of δ_x and δ_z calculated by means of the outer solution, Eq. [6] (dahsed line), and of the inner solution, Eq. [8] (dotted line), are also given. One sees that the compound solution for $x(\varphi)$ (the solid line in Fig. 2a) provides better accuracy in comparison with the inner and the outer solu-

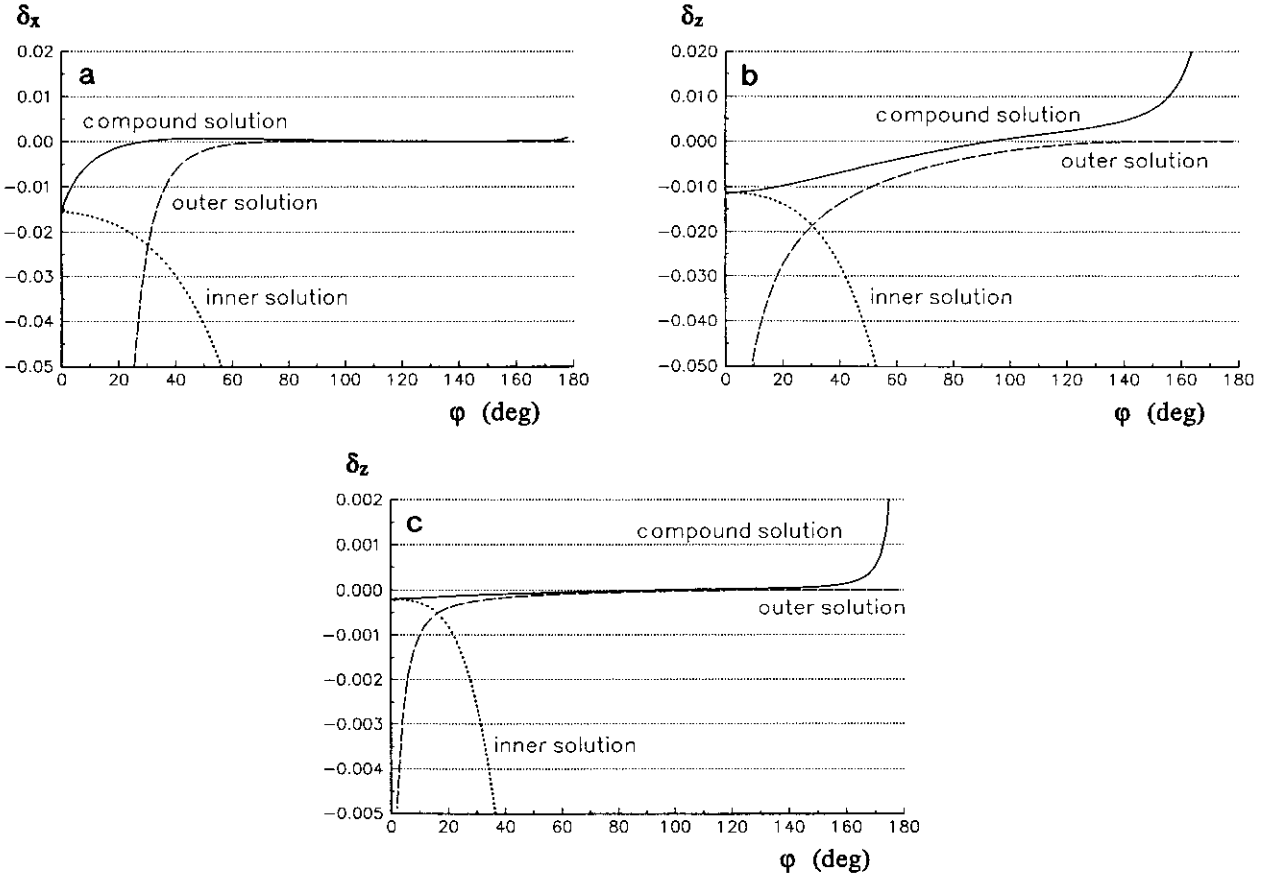

FIG. 2. Relative error of the asymptotic expansions vs running slope angle φ for senssile interface ($\epsilon = 1$): (a) δ_x vs φ for $\beta = 0.1$; (b) δ_z vs φ for $\beta = 0.1$; (c) δ_z vs φ for $\beta = 0.01$.

tions. The outer solution coincides with the compound one in the range for φ from 80° to 180°.

The relative error δ_z calculated by means of Eq. [19] for $\beta = 0.1$ and 0.01 is shown in Figs. 2b and 2c. The comparison between these two figures implies that the accuracy of the asymptotic formulae strongly increases with the decrease of β, as it could be expected. It is seen also that the compound solution for $z(\varphi)$ has better precision than the outer and the inner solutions when $0° \leqslant \varphi \leqslant 110°$. If φ is larger than 110°, the outer solution becomes more precise than the compound one. Similar tendency is observed also in Fig. 2a for δ_x, where the compound solution coincides with the outer solution for φ in the range 80–170°. That is why we suggest to the reader to use the compound solution for $x(\varphi)$ and $z(\varphi)$ when $\varphi \leqslant 110°$ and the respective outer solutions when $\varphi > 110°$.

Four curves of constant error $|\delta_x| = 0.01$, 0.001, 10^{-4}, and 10^{-5} calculated from Eq. [18] (where the compound solution is used for $\varphi \leqslant 110°$ and the outer one—for $\varphi > 110°$) are plotted in Fig. 3a. The same calculations are made for δ_z by means of Eq. [19] and the results are shown in Fig. 3b. For all points below a given curve the precision of the asymptotic solution is higher than the one corresponding to this curve. The curves have a small break at $\varphi = 110°$, which is due to the transition from the compound to the outer solution. The curves in Fig. 3a have a peak around $\varphi \approx 30°$, because in this region δ_x changes sign—cf. Fig. 2a. The curves in Fig. 3b have the same peak around $\varphi \approx 90°$. The curves β vs φ in Fig. 3 sharply increase when $\varphi \to 180°$, because then the outer asymptotic solution tends to the exact shape (see Ref. (10)).

One sees in Fig. 2 that at $\varphi = 0$ the compound solution is equal to the inner one. For this point it is easy to derive the following equations by substituting $\varphi = 0$ in Eqs. [8] and [9]:

$$\bar{x}^{in}(\varphi = 0) = \sqrt{\frac{2}{3}\beta(1-\beta)} \qquad [20]$$

$$\bar{z}^{in}(\varphi = 0) = 2 - \beta\left(1 - \frac{1}{2}\ln\frac{\beta}{6}\right). \qquad [21]$$

In the case of a gas bubble attached beneath a horizontal solid surface Eqs. [20] and [21] represent the minimum possible contact radius and the maximum possible height, respectively.

(b) Pendant Interface ($\epsilon = -1$)

There are two possibilities for the parameter η in this case: $\eta = 1$ for $z(\varphi) < z(\varphi_i)$ and $\eta = -1$ for $z(\varphi) > z(\varphi_i)$. The minimum value of φ, φ_i, can be calculated by means of Eq. [11]. To visualize that $z(\varphi)$ is a double-valued function in a vicinity of the inflectional point $\varphi = \varphi_i$ we plotted φ vs z—see the insets in Fig. 4. Since δ_x and δ_z are also double-valued functions of φ, in Fig. 4, we plotted δ_x and δ_z for pendant interfaces as functions of the dimensionalized z-coordinate, z/b.

One sees in Fig. 4a that for $z/b < 2.0$ ($\beta = 0.1$) the error δ_x of the compound solution is very small. In the region $2.0 < z/b < z(\varphi_i)/b$, δ_x is relatively high. Around the inflectional point, $z(\varphi) = z(\varphi_i)$, δ_x increases very fast and goes to infinity. This is due to the fact that the denominator in Eq. [8] equals zero for $\varphi = \varphi_i$ and $\epsilon = -1$.

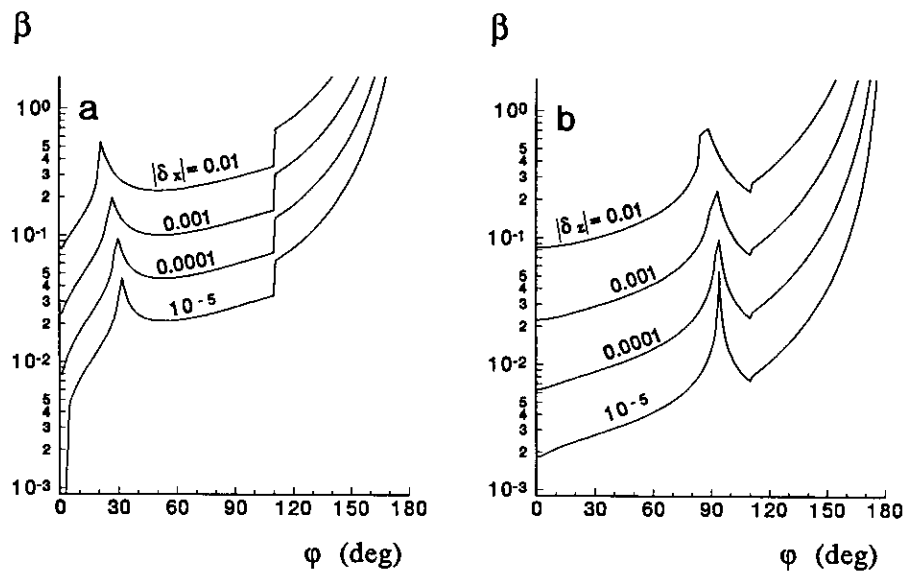

FIG. 3. Curves of constant relative error for sessile interface calculated from the compound expansion for $0° < \varphi < 110°$ and from the outer expansion for $110° < \varphi < 180°$: (a) $|\delta_x|$ = constant; (b) $|\delta_z|$ = constant. For all points below a given curve the relative error is smaller than that corresponding to the curve.

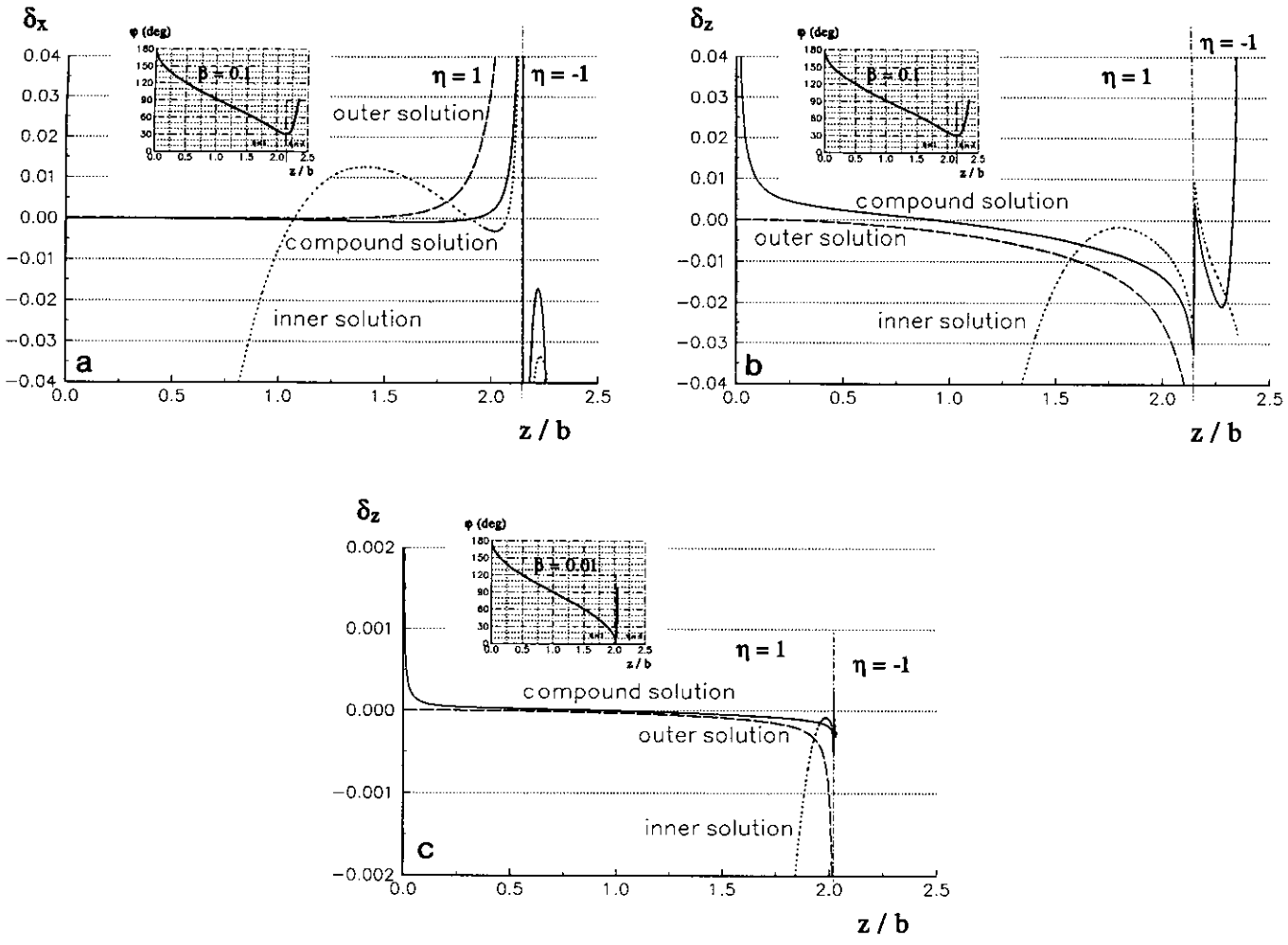

FIG. 4. Relative error of the asymptotic expansions vs z/b for pendant interface ($\epsilon = -1$): (a) δ_x vs z/b for $\beta = 0.1$; (b) δ_z vs z/b for $\beta = 0.1$; (c) δ_z vs z/b for $\beta = 0.01$. The insets represent the exact dependence of the running slope angle φ on z/b calculated numerically for the respective values of β.

The calculated values of δ_z for $\beta = 0.1$ are given in Fig. 4b. It is seen that at the interface apex ($z = 0$) the compound solution provides very large error and similarly to the sessile interface we suggest that the outer solution be used for $\varphi > 110°$ and the compound solution for $\varphi < 110°$. It is interesting to note that at the same value of β the asymptotic solution for $z(\varphi)$ has a smaller error than the respective solution for $x(\varphi)$ in the region $z(\varphi) \geqslant z(\varphi_i)$ (i.e., $\eta = -1$)—cf. Figs 4a and 4b. On the other hand, a comparison between Figs. 4b and 4c shows a pronounced increase in precision when β is decreased. In addition, the problematic region where $\eta = -1$ ($z > z(\varphi_i)$) shrinks with the decrease of β and becomes physically insignificant—cf. the insets in Figs. 4b and 4c. For example, a change in the angle φ from φ_i to 90° in Fig. 4b ($\beta = 0.1$) at $\eta = -1$ corresponds to a change in z/b from 2.15 to 2.35, whereas in Fig. 4c ($\beta = 0.01$ and all other conditions the same) z/b changes from 2.02 to 2.04.

In contrast with $\bar{x}^{in}(\varphi_i)$, the value of $\bar{z}^{in}(\varphi_i)$ is restricted. From Eqs. [9]–[11] for $\epsilon = -1$ one obtains

$$z_i^{in}(\varphi_i) = 2 - \frac{1}{3}\beta \ln\frac{\beta}{6} \qquad [22]$$

In Table 1 we checked the precision of Eqs. [11] and [22] determining φ_i and z_i (parameters of the inflectional point

TABLE 1
Numerical Test of Eqs. [11] and [22] against Exact Computer Solution

β	φ_i(°) Eq. [11]	φ_i(°) exact	$\bar{z}(\varphi_i)$ Eq. [22]	$\bar{z}(\varphi_i)$ exact
10^{-1}	29.59	30.94	2.1365	2.1494
3×10^{-2}	16.21	16.69	2.0530	2.0564
10^{-2}	9.36	9.40	2.0213	2.0211
3×10^{-3}	5.37	5.37	2.0076	2.0075
10^{-3}	2.96	2.96	2.0029	2.0029
3×10^{-4}	1.62	1.62	2.0010	2.0010
10^{-4}	0.94	0.94	2.0004	2.0004

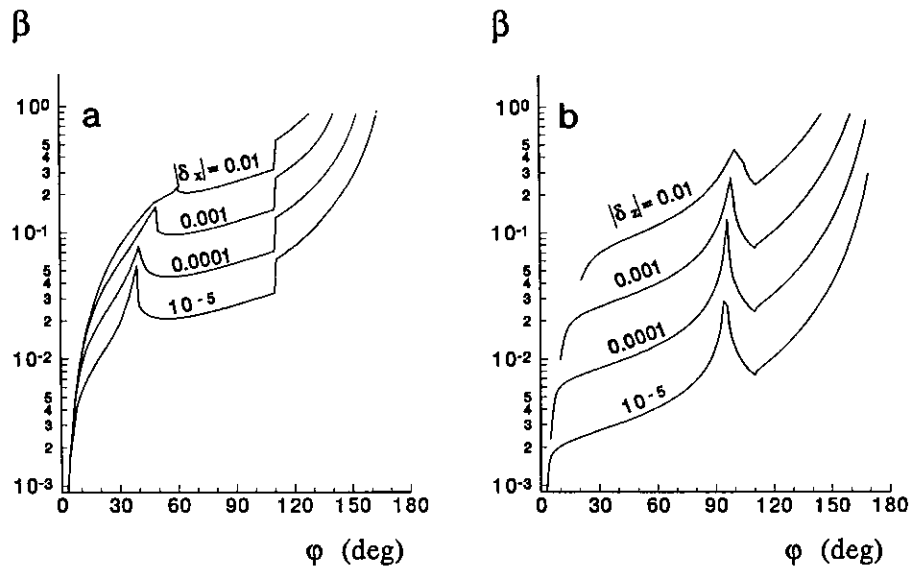

FIG. 5. Curves of constant relative error for pendant interface calculated from the compound expansion for $0° < \varphi < 110°$ and from the outer expansion for $110° < \varphi < 180°$: (a) $|\delta_x|$ = constant; (b) $|\delta_z|$ = constant. For all points below a given curve the relative error is smaller than that corresponding to the curve.

in the pendant drop profile) against the exact values of these parameters calculated by means of numerical investigation of Laplace equation. As it is to be expected, Eqs. [11] and [23] are more accurate for smaller values of β. It should be noted that the accuracy of our compound solution is the worst in a vicinity of the inflection point of the pendant interface, illustrated numerically in Table 1. For larger values of φ the accuracy fast improves and the compound solution becomes practically exact at the fluid particle equator ($\varphi = 90°$), even for $\beta = 0.1$—see Figs. 2a, b and 4a, b.

Figures 5a and 5b represent curves of constant error for pendant interfaces. Figure 5a relates to constant $|\delta_x|$ and Fig. 5b to constant $|\delta_z|$. We plotted in Fig. 5 only the data calculated with $\eta = 1$. The breaking of the curves at $\varphi = 110°$ is due to the transition from the outer to the compound solution. The peaks of the curves in Fig. 5a appear around 40–50° where δ_x changes sign, and the peaks of the curves in Fig. 5b appears around $\varphi \approx 90°$ where δ_z changes sign.

4. CONCLUDING REMARKS

In the present article we derived a *compound* asymptotic expansion describing the shape of sessile and pendant liquid–fluid interfaces by matching the *outer* and *inner* expansions previously derived in Ref. (10). Here we pay attention to the case of a pendant interface, which has not been considered in detail in Ref. (10). In these aspects the present paper is a continuation and complement of the study in Ref. (10).

The expansions are derived for small values of the Bond number, β, defined by Eq. [1]. For small β the droplet (bubble) surface is almost spherical except the region of slope angles $0 < \varphi < 30°$ (see Fig. 1), where the gravitational deformation is significant. Figures 2 and 4 show that the *compound* expansion derived here has a considerably better accuracy in the region $0 < \varphi < 30°$ compared to the *outer* and *inner* expansions. In fact, the compound expansion has the best precision for all values of φ ($0 < \varphi < 180°$), excluding a small vicinity of the fluid particle apex ($\varphi = 180°$), where the outer expansion is more precise.

This study was provoked by the experiments on contact angle and line tension measurements with small bubbles attached to a liquid–gas interface (13–16). In these experiments the slope at the contact line belongs to the interval $0 < \varphi < 20°$. This ie exactly the region where our compound expansion provides the greatest improvement over the outer and inner expansions—see Fig. 2.

We hope the compound analytical expansions, Eqs. [16] and [17], can find application for experimental data interpretation in any case, when the slope angle φ at the contact line of small fluid particles is between 0° and 30°. These can be floating bubbles and oil droplets; bubbles or droplets pressed by the upthrust beneath a solid plate; or sessile droplets forming large contact angles like water droplet on strongly hydrophobic substrate, mercury droplet on glass, etc.

ACKNOWLEDGMENT

This work was supported by the Research and Development Corporation of Japan (JRDC) under the program "Exploratory Research for Advanced Technology" (ERATO).

REFERENCES

1. Adamson, A. W., "Physical Chemistry of Surfaces." Wiley, New York, 1976.

2. Hartland, S., and Hartley, R. W., "Axisymmetric Fluid–Liquid Interfaces." Elsevier, Amsterdam, 1976.
3. Padday, J. F., *in* "Surface and Colloid Science" (E. Matijevič, Ed.), Vol. 1, p. 39. Wiley, New York, 1969.
4. Princen, H. M., *in* "Surface and Colloid Science" (E. Matijevič and F. R. Eirich, Eds.), Vol. 2, p. 1. Wiley, New York, 1969.
5. Cheng, P., Li, D., Boruvka, L., Rotenberg, Y., and Neumann, A. W., *Colloids Surf.* **43,** 151 (1990).
6. Skinner, F. K., Rotenberg, Y., and Neumann, A. W., *J. Colloid Interface Sci.* **130,** 25 (1989).
7. Dimitrov, A. S., Kralchevsky, P. A., Nikolov, A. D., and Wasan, D. T., *Colloids Surf.* **47,** 299 (1990).
8. Dimitrov, A. S., Kralchevsky, P. A., Nikolov, A. D., Noshi, H., and Matsumoto, M., *J. Colloid Interface Sci.* **145,** 279 (1991).
9. Concus, P., *J. Fluid Mech.* **34,** 481 (1968).
10. Kralchevsky, P. A., Ivanov, I. B., and Nikolov, A. D., *J. Colloid Interface Sci.* **112,** 108 (1986).
11. Nayfeh, A. H., "Perturbation Methods." Wiley, New York, 1973.
12. Forsyte, G. E., Malcolm, M. A., and Moler, C. B., "Computer Methods for Mathematical Computations." Prentice–Hall, Englewood Cliffs, NJ, 1977.
13. Kralchevsky, P. A., Nikolov, A. D., and Ivanov, I. B., *J. Colloid Interface Sci.* **112,** 132 (1986).
14. Lobo, L. A., Nikolov, A. D., Dimitrov, A. S., Kralchevsky, P. A., and Wasan, D. T., *Langmuir* **6,** 995 (1990).
15. Ivanov, I. B., Dimitrov, A. S., Nikolov, A. D., Denkov, N. D., and Kralchevsky, P. A., *J. Colloid Interface Sci.* **151,** 446 (1992).
16. Dimitrov, A. S., Nikolov, A. D., Kralchevsky, P. A., and Ivanov, I. B., *J. Colloid Interface Sci.* **151,** 462 (1992).